South East Asian J. of Mathematics and Mathematical Sciences Vol. 20, No. 3 (2024), pp. 463-478

ISSN (Print): 0972-7752

INFLUENCE OF SLIP VELOCITY AND VARIATIONS IN BLOOD VISCOSITY ON BLOOD FLOW IN A DISEASED ARTERY CHARECTERIZED BY TIME DEPENDENT STENOSIS

Lovely Jain and Samarth Srivastava

Department of Mathematics, Amity Institute of Applied Sciences, Amity University, Noida - 201301, Uttar Pradesh, INDIA

E-mail: luvlyjain@gmail.com, samarth.s2003@gmail.com

(Received: Jan. 11, 2024 Accepted: Dec. 20, 2024 Published: Dec. 30, 2024)

Abstract: The aim of this paper is to investigate the effect of slip velocity and axial variation in blood viscosity on the flow dynamics within an artery characterized by time-dependent stenosis. The blood viscosity is found to be contingent upon the axial coordinate, leading to an ascending viscosity trend towards the highest point of stenosis, followed by a subsequent descent. Employing analytical methodologies, this study delves into the intricacies of the issue, deriving equations governing volumetric flow rate, flow resistance, axial velocity and shearing stress on wall. Notably, an increase in the stenosis height correlates with heightened flow resistance and augmented wall shear stress. The novelty of this study lies in its comprehensive approach to modeling the simultaneous effects of slip velocity and variable blood viscosity in a time-varying stenosed artery, a topic previously unexplored.

Keywords and Phrases: Time-dependent stenosis, resistance to flow, shearing stress on wall, slip velocity, blood viscosity, flow of blood.

2020 Mathematics Subject Classification: 92B05, 92C10, 92C35.

Nomenclature

(-t/T) Dimensionless time

 α Index of viscosity variation

 δ Height of stenosis

 λ Resistance to flow

 λ_k Dimensionless resistance to flow

 $\mu(z)$ Viscosity of fluid

R(z,t) Distance between stenosis and center

 τ_w Wall shear stress

 $\hat{\tau_w}$ Dimensionless Wall shear stress

L Length of artery

 L_0 Length of stenosis

 L_1 Length of inlet zone

p Fluid pressure

Q Volumetric rate of flow

r Radial distance

 R_0 Normal Radius of artery

u Axial velocity

 u_s Slip velocity

z Axial distance

1. Introduction

A human artery's lumen can develop stenosis, an abnormal and unnatural growth. A diameter decrease ranging from 60–75% of the major problematic artery is typically thought of as a critical stenosis. To deal with such a high level of stenosis, certain medical procedures like balloon angioplasty, placement of a stent, or arterial bypass grafting are carried out.

There have been various studies flow of blood through a mildly stenotic artery using mathematical models which analyze the influence of slip velocity or peripheral plasma layer thickness on wall shear stress, flow resistance, velocity, etc. [2, 3, 19, 9]. The influence of pressure on fluid flow dynamics, such as velocity and flow rate for the non Newtonian Casson fluid flow was investigated by [6] and [11] and the studies report a decline in velocity with an increase in the Casson parameter. The impact of viscosity of blood on the flow of blood and the effect of low molecular weight Dextran were studied by [5]. The existence of a strong inverse relationship between blood flow and changes in viscosity, the latter being three times greater

2. Formation and Analysis of Model

A steady blood flow of Newtonian, homogeneous blood is considered in a time-dependent mild stenotic artery under slip velocity condition. The stenosis is axisymmetrical, one-dimensional and is dependent upon z, the axial distance. Blood is divided into three zones i.e., inlet, stenotic and outlet zone with the stenotic zone being the site for the accumulation of red blood cells.

On the basis of the geometry of the stenosis, the radius of an artery in the stenotic region can be expressed as follows:

$$\frac{R(z,t)}{R_0} = \begin{cases}
1 - \frac{\sigma(1 - e^{-t/T})}{2R_0} \left\{ 1 + \cos\frac{2\pi}{L_0} \left(z - L_1 - \frac{L_0}{2} \right) \right\}, L_1 \le z \le L_1 + L_0 \\
1, \qquad 0 \le z \le L_1, L_0 + L_1 \le z \le L
\end{cases} \tag{1}$$

Where L_0 denotes the stenosis length and σ indicates the highest point of the

stenosis, which is thought to be much lower than the artery's radius. ($\sigma \ll R_0$). The equation of one dimensional flow motion with viscosity as function of axial distance, z, is given by,

$$0 = -\frac{dp}{dz} + \frac{\mu(z)}{r} \frac{d}{dr} \left\{ r \frac{du}{dr} \right\}$$
 (2)

Here, axial velocity is denoted by u, fluid pressure by p, and $\mu(z)$ denotes viscosity as function of z. It is given as follows [7]:

$$\mu(z,t) = \begin{cases} \mu_1 \left(\frac{R(z,t)}{R_0}\right)^{-\alpha}, & L_1 \le z \le L_1 + L_0\\ \mu_1, & 0 \le z \le L_1 \text{ and } L_0 + L_0 \le z \le L \end{cases}$$
(3)

for $\alpha = 0, 1, 2, 3...$

Here, viscosity of fluid, which is constant is represented by μ_1 and α index of viscosity variation which is an arbitrary parameter. The above mathematical representation of viscosity variation is quite realistic as accumulation of blood cells when the radius becomes minimum and viscosity maximum, ahead of the minimum gap.

The boundary wall condition associated with equation (2) are listed below:

$$\frac{du}{dr} = 0 \text{ at } r = 0 \tag{4}$$

$$u = u_s$$
 at $r = R(z, t)$ (5)

On solving equation (1) using equations (4) and (5) we get the velocity function u':

$$u' = u_{\rm s} - \frac{1}{4\mu} \frac{dp}{dz} (R^2 - r^2) \tag{6}$$

The volumetric rate of flow Q through the arterial segment is given by [13]:

$$Q = \int_0^R 2\pi r u' dr \tag{7}$$

Upon solving equation (7) by integrating within limits 0 to R, we get:

$$Q = \pi R^2 u_{\rm s} - \frac{\pi R^4}{8\mu} \frac{dp}{dz} \tag{8}$$

From equation (8), it is possible to determine the pressure gradient as

$$\frac{dp}{dz} = \frac{8\mu}{\pi R^4} \left(\pi R^2 u_{\rm s} - Q \right) \tag{9}$$

Integrating equation (9) subject to condition $p = p_0$ at z = 0 and $p = p_L$ at z = L we have,

$$\Delta p = p_0 - p_L = \frac{8G}{\pi} \left(Q - \pi R^2 u_s \right)$$
 (10)

where

$$G = \int_0^L \frac{\mu(z, t)}{R^4}$$
 (11)

2.1. Methodology to obtain Resistance to Flow

The resistance to flow (λ) , which has a physiological importance, is obtained using the methodology explained below [7],

$$\lambda = \frac{\Delta p}{Q} = \frac{8G}{\pi} - \frac{8GR^2 u_{\rm s}}{Q} \tag{12}$$

Where ΔP is the difference between the pressure at the entry and exit level respectively.

Now, we can rewrite the value of λ using the idea of viscosity variation given by (3) as follows:

$$\lambda = \frac{8\mu_1}{\pi R_0^4} \left[L - L_0 + \int_{L_1}^{L_1 + L_0} \frac{dz}{\left(\frac{R(z,t)}{R_0}\right)^{4+\alpha}} \right] - \frac{8\mu_1 u_s}{Q R_0^2} \left[L - L_0 + \int_{L_1}^{L_1 + L_0} \frac{dz}{\left(\frac{R(z,t)}{R_0}\right)^{4+\alpha}} \right]$$
(13)

The effect of viscosity variation on the peripheral resistance is given by equation (13). $\alpha = 0$ denotes the case for constant viscosity and the result is the same as given by [21]. It can be interpreted from equation (13) that an increase in the value of α causes the peripheral resistance to flow to increase up to the highest stenosis height possible for a stenosis of fixed size. Moreover, the variation in value of λ with the height of stenosis implies that an increase in the height of stenosis causes the peripheral resistance to increase. Taking λ_k as the non-dimensionalised resistance to flow, we consider the following 3 cases to study the effect of α on λ : For $\alpha = 0$

$$\lambda_{k} = \frac{\lambda_{0}}{\lambda_{0}'} = \left(1 - \frac{u_{s}\pi R_{0}^{2}}{Q}\right)^{-1} \left(A_{0} - \frac{u_{s}\pi R_{0}^{2}}{Q}B_{0}\right)$$

Where
$$A_0 = \left[1 - \frac{L_0}{L} + \frac{L_0}{L} \left(1 - \frac{\delta}{R_0} (e^{-t/T} - 1)\right)^{-7/2} \left(1 - \frac{\delta}{2R_0} (e^{-t/T} - 1)\right)\right]$$

$$\left(\frac{5}{8} \frac{\delta^2}{R_0^2} (e^{-t/T} - 1)^2 - \frac{\delta}{R_0} (e^{-t/T} - 1) + 1\right)\right]$$

$$B_0 = \left[1 - \frac{L_0}{L} + \frac{L_0}{L} \left(1 - \frac{\delta}{2R_0} (e^{-t/T} - 1)\right) \left(1 - \frac{\delta}{R_0} (e^{-t/T} - 1)\right)^{-3/2}\right]$$
and $\lambda_0' = \frac{8\mu_1 L}{\pi R_0^4} \left(1 - \frac{u_s \pi R_0^2}{Q}\right)$ (14)

For $\alpha = 1$

$$\lambda_{k} = \frac{\lambda_{1}}{\lambda_{1}'} = \left(1 - \frac{u_{s}\pi R_{0}^{2}}{Q}\right)^{-1} \left(A_{1} - \frac{u_{s}\pi R_{0}^{2}}{Q}B_{1}\right)$$
Where $A_{1} = \left[1 - \frac{L_{0}}{L} + \frac{L_{0}}{4L}\left(1 - \frac{\delta}{R_{0}}(e^{-t/T} - 1)\right)^{-9/2} \left(8\left(1 - \frac{\delta}{2R_{0}}(e^{-t/T} - 1)\right)^{2} + 3\left(\frac{\delta}{R_{0}}(e^{-t/T} - 1)\right)^{2} \left(8\left(1 - \frac{\delta}{2R_{0}}(e^{-t/T} - 1)\right)^{2} + 1\right)\right];$

$$B_{1} = \left[1 - \frac{L_{0}}{L} + \frac{L_{0}}{L}\left(1 - \frac{\delta}{R_{0}}(e^{-t/T} - 1)\right)^{-5/2} \left(\frac{3}{2}\left(\frac{\delta}{2R_{0}}(e^{-t/T} - 1)\right)^{2} - 2\left(\frac{\delta}{2R_{0}}(e^{-t/T} - 1)\right) + 1\right)\right]; \text{ and } \lambda_{1}' = \frac{8\mu_{1}L}{\pi R_{0}^{4}}\left(1 - \frac{u_{s}\pi R_{0}^{2}}{Q}\right) \quad (15)$$

For $\alpha = 2$

$$\lambda_{k} = \frac{\lambda_{2}}{\lambda_{2}'} = \left(1 - \frac{u_{s}\pi R_{0}^{2}}{Q}\right)^{-1} \left(A_{2} - \frac{u_{s}\pi R_{0}^{2}}{Q}B_{2}\right)$$
Where $A_{2} = \left[1 - \frac{L_{0}}{L} + \frac{L_{0}}{4L}\left(1 - \frac{\delta}{2R_{0}}(e^{-t/T} - 1)\right)\left(1 - \frac{\delta}{R_{0}}(e^{-t/T} - 1)\right)^{-11/2}\right]$

$$\left[4\left(1 - \frac{\delta}{2R_{0}}(e^{-t/t} - 1)\right)^{4} + 20\left(1 - \frac{\delta}{2R_{0}}(e^{-t/t} - 1)\right)^{2}\left(\frac{\delta}{2R_{0}}(e^{-t/T} - 1)\right)^{4} + \frac{15}{2}\left(\frac{\delta}{2R_{0}}(e^{-t/T} - 1)\right)^{4}\right]\right];$$

Influence of slip Velocity and Variations in Blood Viscosity on Blood Flow ... 469

$$B_{2} = \left[1 - \frac{L_{0}}{L} + \frac{L_{0}}{L} \left(1 - \frac{\delta}{2R_{0}} (e^{-t/T} - 1)\right) \left(1 - \frac{\delta}{R_{0}} (e^{-t/T} - 1)\right)^{-7/2} \left(\frac{5\delta^{2}}{8R_{0}^{2}} (e^{-t/T} - 1)^{2} - \frac{\delta}{R_{0}} (e^{-t/T} - 1) + 1\right)\right]; \text{ and } \lambda_{1}' = \frac{8\mu_{1}L}{\pi R_{0}^{4}} \left(1 - \frac{u_{s}\pi R_{0}^{2}}{Q}\right)$$

$$(16)$$

2.2. Methodology to obtain Wall shear stress

The shear stress at the wall is obtained by the following relation [7];

$$\tau_{\rm w} = -\mu(z, t) \frac{dw}{dr} \bigg|_{r=R(z,t)} \tag{17}$$

Using equation (9) and equation (3) we have,

$$\tau_{\rm w} = \frac{4Q\mu_1}{\pi R^3} \left(\frac{R(z,t)}{R_0}\right)^{-\alpha-3} - \frac{4\mu_1 u_{\rm s}}{R} \left(\frac{R(z,t)}{R_0}\right)^{-\alpha-1}$$
(18)

Using the above equation and substituting the value of R, the shear stress at the maximum stenosis height can be achieved. This is represented by equation (19)

$$\tau_{\rm w} = \frac{4Q\mu_1}{\pi R^3} \left(1 - \frac{\delta}{R_0} (e^{-t/T} - 1) \right)^{-\alpha - 3} - \frac{4\mu_1 u_{\rm s}}{R} \left(1 - \frac{\delta}{R_0} (e^{-t/T} - 1) \right)^{-\alpha - 1}$$
(19)

or,

$$\hat{\tau_{w}} = \frac{\tau_{w} \pi R_{0}^{3}}{4Q\mu_{1}} = \left(1 - \frac{\pi u_{s} R_{0}^{2}}{Q}\right)^{-1} \left[\left(1 - \frac{\delta}{R_{0}} (e^{-t/T} - 1)\right)^{-\alpha - 3} - \frac{\pi u_{s} R_{0}^{2}}{Q} \left(1 - \frac{\delta}{R_{0}} (e^{-t/T} - 1)\right)^{-\alpha - 1} \right]$$
(20)

For $\alpha=0$, we arrive at the constant viscosity condition and the results obtained are identical to Young (1968). Based on equation (20), it can be concluded that an increase in the value of alpha causes the wall shear stress to increase up to the highest stenosis height possible for a fixed stenosis size. Moreover, it is seen that an increase in the height of stenosis causes an increase in the wall shear stress as well. We consider the following 3 cases to study the effect of α on τ : For $\alpha=0$

$$\hat{\tau_{\mathbf{w}}} = \frac{\tau_{\mathbf{w}} \pi R_0^3}{4Q\mu_1} = \left(1 - \frac{\pi u_{\mathbf{s}} R_0^2}{Q}\right)^{-1} \left[\left(1 - \frac{\delta}{R_0} (e^{-t/T} - 1)\right)^{-3} - \right]$$

$$\frac{\pi u_{\rm s} R_0^2}{Q} \left(1 - \frac{\delta}{R_0} (e^{-t/T} - 1) \right)^{-1}$$
 (21)

For $\alpha = 1$

$$\hat{\tau_{w}} = \frac{\tau_{w} \pi R_{0}^{3}}{4Q\mu_{1}} = \left(1 - \frac{\pi u_{s} R_{0}^{2}}{Q}\right)^{-1} \left[\left(1 - \frac{\delta}{R_{0}} (e^{-t/T} - 1)\right)^{-2} - \frac{\pi u_{s} R_{0}^{2}}{Q} \right]$$
(22)

For $\alpha = 2$

$$\hat{\tau_{w}} = \frac{\tau_{w} \pi R_{0}^{3}}{4Q\mu_{1}} = \left(1 - \frac{\pi u_{s} R_{0}^{2}}{Q}\right)^{-1} \left[\left(1 - \frac{\delta}{R_{0}} (e^{-t/T} - 1)\right)^{-1} - \frac{\pi u_{s} R_{0}^{2}}{Q} \left(1 - \frac{\delta}{R_{0}} (e^{-t/T} - 1)\right) \right]$$
(23)

3. Results and Discussions

In this section, the implication and influence of the physical parameters of the flow are discussed theoretically and represented graphically. The calculations are carried out analytically and the graphs are plotted using Matlab. Our calculations and graphs are validated for cases with $\alpha = 0$ (special case of no slip velocity condition) by comparing them with already published work of [21]. The expression for λ_k given by Eq. (14) - (16) have been determined for several variables and are graphically represented in figures numbered 2-11. Figure 2 represents the change in resistance of blood to flow as the height of stenosis increases for various lengths of stenosis in the case of constant viscosity. Figures 4 and 6 show the change in flow resistance as the stenosis height increases for different stenosis lengths for alpha = 1, 2. These figures indicate that when the value of length of stenosis if fixed, an increase in the height of stenosis causes the resistance to increase. Furthermore, an increase in the ratio of stenosis length causes the resistance to flow to increase as well. Figure 3 represents the change in resistance to flow as the stenosis height increases for distinct parameters of time in the case of constant viscosity. Figures 5 and 7 represent the flow resistance variation as the stenosis height increases for various parameters of dimensionless time for alpha = 1, 2. On the basis of these graphs, it can be deduced that for an inalterable value of dimensionless time, the flow resistance increases with an increase in the height of stenosis. Furthermore, it is observed that an increase in the dimensionless time causes an increase in the resistance to flow. The variation of resistance to flow with stenosis height for different values of slip velocity is shown through figures 8-11. It can be seen that

an increase in value of slip velocity causes an increase in the resistance to flow. The variation of resistance to flow with stenosis height for different values of alpha is shown in figure 11. Eq. (21)-(23) are plotted in figures 12-14. Figure 12 shows the variation of wall shear stress with stenosis height for different parameters of time in the case of constant viscosity. Figures 13 and 14 show how the shearing stress on wall varies with the stenosis height for alpha = 1, 2. It is observed that an increase in height of stenosis causes the shearing stress on wall to increase. Moreover, as the value of non-dimensionalised time t/T increases, the wall shear stress increases. The effect of different values of slip velocity on variation of wall shear stress with stenosis height can be seen in figures 15-17. On the basis of these graphs, it can be concluded that an increase in the value of slip velocity causes an increase in the shearing stress on wall. Figure 18 shows the variation of wall shear stress with stenosis height for various values of alpha. A key observation is that an increase in the value of alpha causes the shearing stress on wall to decreases.

ratio of stenosis/alpha	0.05	0.1	0.15	0.2	0.25	0.3
0	1.0369	1.0764	1.1185	1.1637	1.2123	1.2646
1	1.0717	1.1511	1.2391	1.3372	1.4469	1.5701
2	1.1076	1.2309	1.3727	1.5366	1.7270	1.9496

Table 1: Ratio of shearing stress with index of viscosity variation for varying stenosis height

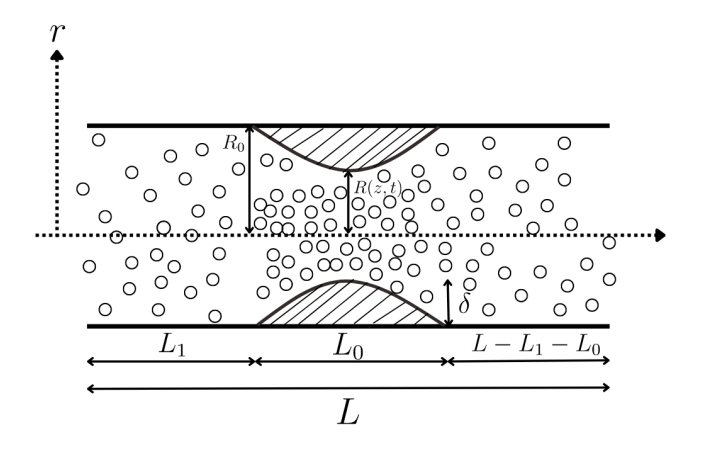


Figure 1: Geometry of the stenosis in an artery

In table 1, slip velocity and time variation is kept constant, and index of viscosity

variation is slowly increased. It is shown that the ratio of shearing stress increases as the severity of stenosis grows. For equal increment in the severity of stenosis, the increase in the ratio of shearing stress is exponential. This is greater in case of a higher index of viscosity variation.

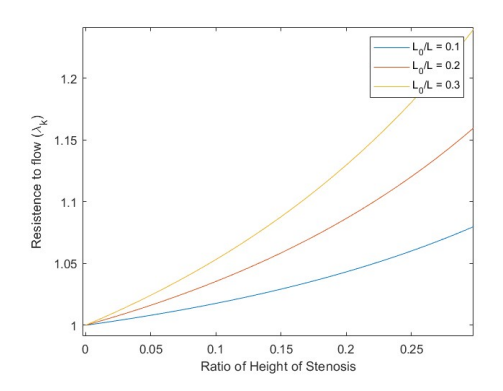


Figure 2: Resistance to flow with stenosis height for different lengths of stenosis when alpha = 0

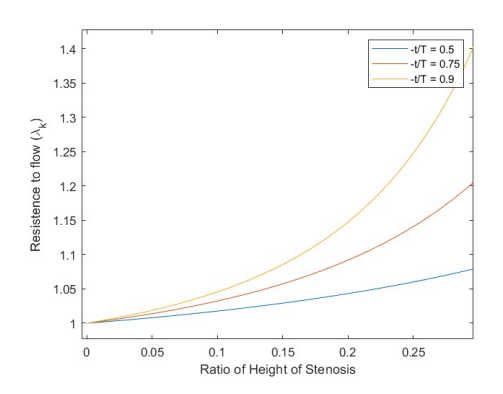


Figure 3: Resistance to flow with stenosis height for different parameters of time when alpha = 0

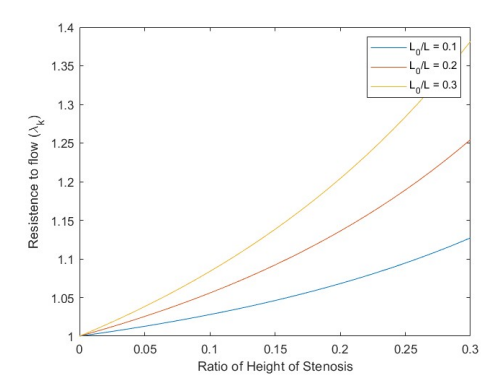


Figure 4: Resistance to flow with stenosis height for different lengths of stenosis when alpha = 1

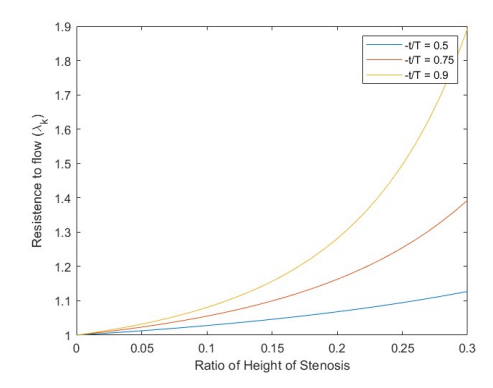


Figure 5: Resistance to flow with stenosis height for different parameters of time when alpha = 1

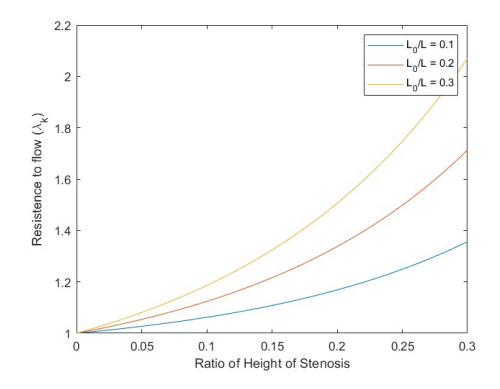


Figure 6: Resistance to flow with stenosis height for different lengths of stenosis when alpha = 2

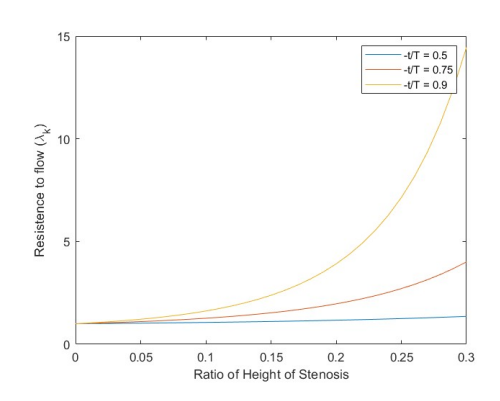


Figure 7: Resistance to flow with stenosis height for different parameters of time when alpha = 2

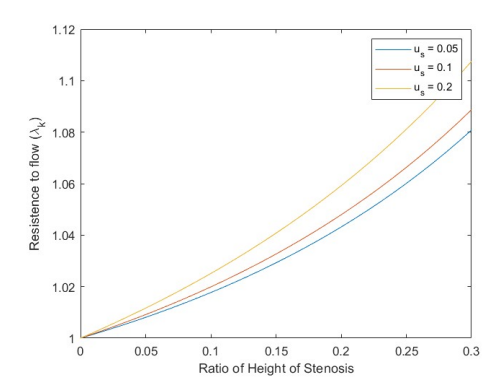


Figure 8: Resistance to flow with stenosis height for different values of slip velocity when alpha = 0

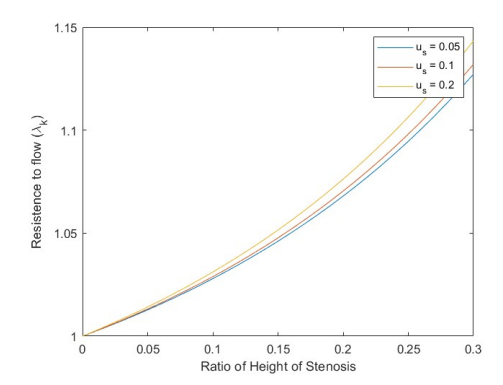


Figure 9: Resistance to flow with stenosis height for different values of slip velocity when alpha = 1

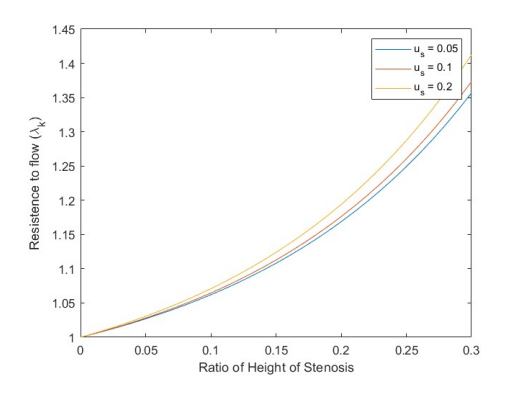


Figure 10: Resistance to flow with stenosis height for different values of slip velocity when alpha = 2

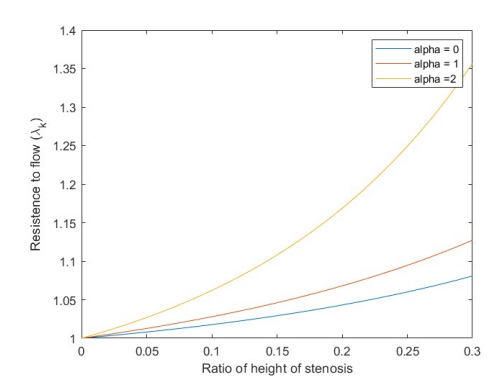


Figure 11: Resistance to flow with stenosis height for different values of alpha

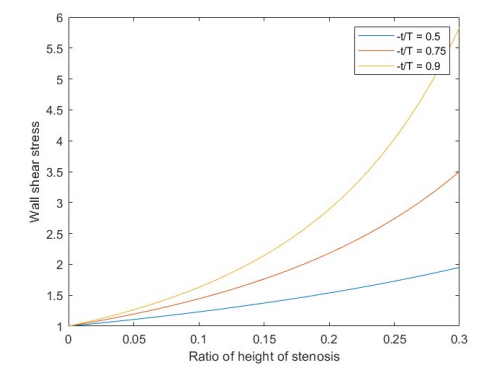


Figure 12: Wall shear stress with stenosis height for different parameters of time when alpha = 0

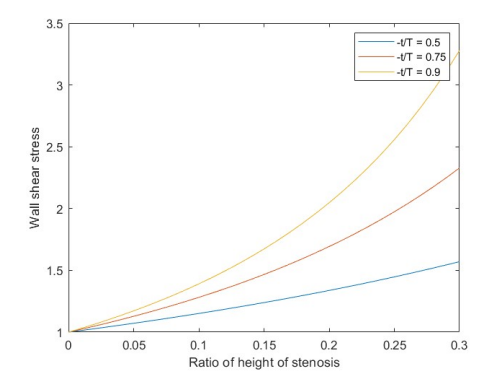


Figure 13: Wall shear stress with stenosis height for different parameters of time when alpha = 1

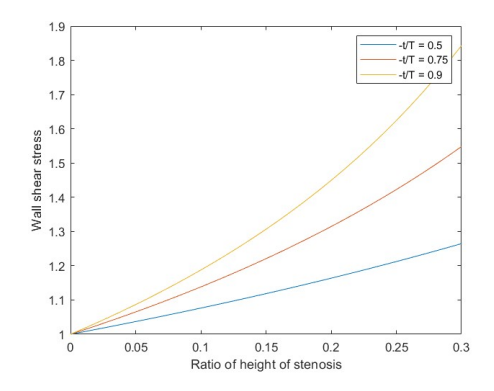


Figure 14: Wall shear stress with stenosis height for different parameters of time when alpha = 2

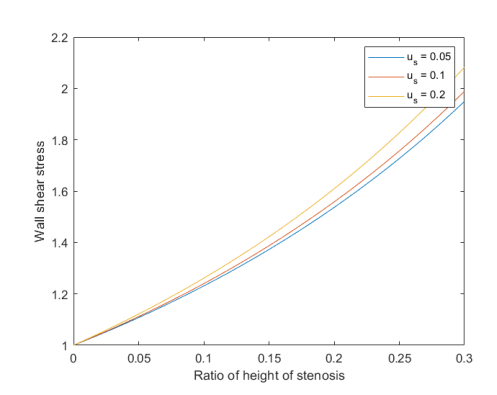


Figure 15: Wall shear stress with stenosis height for different values of slip velocity when alpha = 0

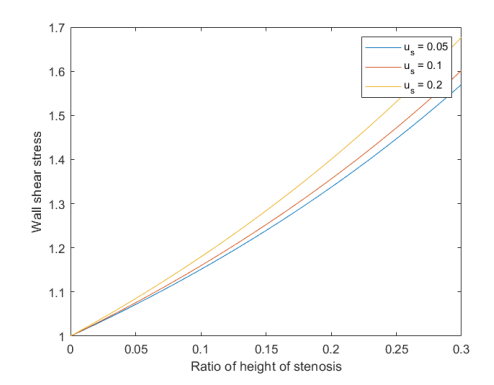


Figure 16: Wall shear stress with stenosis height for different values of slip velocity when alpha = 1

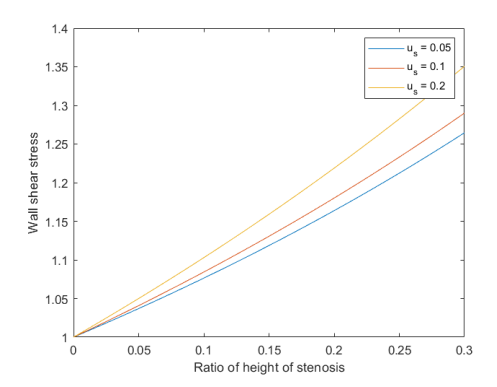


Figure 17: Wall shear stress with stenosis height for different values of slip velocity when alpha = 2

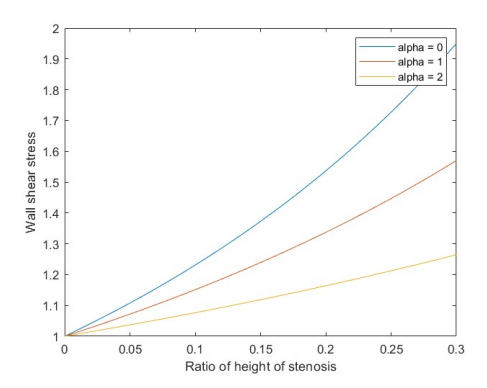


Figure 18: Wall shear stress with stenosis height for different values of alpha

4. Conclusion

The proposed model analyzes the effects of red cells, when aggregated, on the blood flow, causing the viscosity to axially variate in the region of an artery which is time-dependent stenotic. It is found that an increase in the value of non-dimensionalized time t/T, stenosis height or stenosis length is directly proportional to the flow resistance of blood and the wall shear stress. This study analyzes the effect of pressure on the walls of the artery which play a crucial role in the early detection of cerebrovascular and cardiovascular system-related stroke problems. Understanding the into abnormal flow through the relations between resistance to flow and stenosis height can help identify risks of complications like blood clots, aneurysms, or ischemia which can further help tailor treatments depending on the shape and size of the stenosis. We hope the findings presented through this study could be utilized in a more accurate flow detection in bio-medical instruments.

References

- [1] Abbas Z., Mehboob R., Rafiq M. Y., Khaliq S., and Ali A., Peristaltic pumping of ternary hybrid nanofluid between two sinusoidally deforming curved tubes, Advances in Mechanical Engineering, 15(7) (2023), 16878132231189373.
- [2] Chaturani P. and Kaloni P., Two layered poiseuille flow model for blood flow through arteries of small diameter and arterioles, Biorheology, 13(4) (1976), 243–250.
- [3] Chaturani P. and Upadhya V., A two-fluid model for blood flow through small diameter tubes, Biorheology, 16(1-2) (1979), 109–118.

- [4] Deshpande M., Giddens D., and Mabon R., Steady laminar flow through modelled vascular stenoses, Journal of Biomechanics, 9(4) (1976), 165–174.
- [5] Dormandy J. A., Influence of blood viscosity on blood flow and the effect of low molecular weight dextran, Br Med J, 4(5789) (1971), 716–719.
- [6] Fayyaz A., Abbas Z. and Rafiq M. Y., Exploration of the dynamics of heated non-newtonian casson fluid within an annular region of eccentric cylinders subject to peristaltic motion, Proceedings of the Institution of Mechanical Engineers, Part E: Journal of Process Mechanical Engineering, (2024), 09544089241279215.
- [7] Jain L. and Kushwaha M., Effect of blood viscosity variation on the flow of blood in an artery having time dependent stenosis, Contemporary Mathematics, (2023), 675–683.
- [8] Kumar A., Sharma B. K., Bin-Mohsen B., and Fernandez-Gamiz U., Statistical analysis of radiative solar trough collectors for mhd jeffrey hybrid nanofluid flow with gyrotactic microorganism: entropy generation optimization, International Journal of Numerical Methods for Heat & Fluid Flow, 34(2) (2024), 948–979.
- [9] Majhi S. and Usha L., Fahraeus-lindqvist effect and generalized poiseuille flow with or without wall slip, In Proc. 13th Nat. Conf. Fluid Mech. Fluid Power, REC, Thiruchirappalli, India, (1984), 125–128.
- [10] Mishra N. K., Sharma P., Sharma B. K., Almohsen B. and P'erez L. M., Electroosmotic mhd ternary hybrid jeffery nanofluid flow through a ciliated vertical channel with gyrotactic microorganisms: Entropy generation optimization, Heliyon, 10(3), (2024).
- [11] Mujahid M., Abbas Z., and Rafiq M. Y., A study on the pressure-driven flow of magnetized non-newtonian casson fluid between two corrugated curved walls of an arbitrary phase difference, Heat Transfer.
- [12] Perkko J. and Keskinen R., On the effect of the concentration profile of red cells on blood flow in the artery with stenosis, Bulletin of mathematical biology, 45 (1983), 259–267.
- [13] Pokharel C., Gautam P. N., Bhatta C. R., and Kafle J., Analysis of blood flow through stenosed artery with Einstein viscosity, Journal of Tianjin University Science and Technology, 57(4) (2024), 36–52.

- [14] Pontrelli G., Blood flow through an axisymmetric stenosis, Proceedings of the Institution of Mechanical Engineers, Part H: Journal of Engineering in Medicine, 215(1) (2001), 1–10.
- [15] Rafiq M. Y., Sabeen A., Rehman A. U., and Abbas Z., Comparative study of yamada-ota and xue models for mhd hybrid nanofluid flow past a rotating stretchable disk: stability analysis, International Journal of Numerical Methods for Heat & Fluid Flow, 34(10) (2024), 3793–3819.
- [16] Shahzad H., Abbas Z., and Rafiq M., Molecular dynamics study of the thermal radiatively pressure-driven flow of two immiscible hybrid nanofluids through a curved pipe with viscous dissipation, Chaos, Solitons & Fractals, 188 (2024), 115552.
- [17] Sharma B. K., Kumar A., Almohsen B., and Fernandez-Gamiz U., Computational analysis of radiative heat transfer due to rotating tube in parabolic trough solar collectors with darcy forchheimer porous medium, Case Studies in Thermal Engineering, 51 (2023), 103642.
- [18] Sharma B. K., Kumar A., Mishra N. K., Albaijan I., and Fernandez Gamiz U., Computational analysis of melting radiative heat transfer for solar riga trough collectors of jeffrey hybrid-nanofluid flow: a new stochastic approach, Case Studies in Thermal Engineering, 52 (2023), 103658.
- [19] Shukla J., Parihar R., and Gupta S., Effects of peripheral layer viscosity on blood flow through the artery with mild stenosis, Bulletin of Mathematical Biology, 42 (1980), 797–805.
- [20] Umar F. M. and Ali M., Evaluation of the effect of viscosity on blood flow using viscosity models, Dutse Journal of Pure and Applied Sciences, 10(3c) (2024), 230–234.
- [21] Young D. F., Effect of a time-dependent stenosis on flow through a tube, Journal of Engineering for Industry, 90(2) (1968), 248–254.